

Core Collapse Via Coarse Dynamic Renormalization

Andras Szell and David Merritt

Rochester Institute of Technology, 54 Lomb Memorial Drive, Rochester, NY 14623

Ioannis G. Kevrekidis

Department of Chemical Engineering and Program in Applied and Computational Mathematics, Princeton University, Princeton, NJ 08544

(Dated: January 20, 2018)

In the context of the recently developed “equation-free” approach to computer-assisted analysis of complex systems, we extract the self-similar solution describing core collapse of a stellar system from numerical experiments. The technique allows us to side-step the core “bounce” that occurs in direct N -body simulations due to the small- N correlations that develop in the late stages of collapse, and hence to follow the evolution well into the self-similar regime.

PACS numbers: Valid PACS appear here

I. INTRODUCTION

In many areas of current research, physical models are available at a fine, microscopic scale, while the questions of most interest concern the system behavior on a coarse-grained, macroscopic level. An example is the gravitational N -body problem [1]. Coarse-grained approximations exist, e. g. the orbit-averaged Fokker-Planck equation [2], which approximates the full $6N$ equations of motion by a differential operator that acts on the single-particle distribution function f . But the derivation of the Fokker-Planck equation from the full N -body equations of motion requires a number of approximations. The “equation-free” computational framework [3, 4, 5] has recently been proposed for the computer-assisted study of such problems, circumventing the derivation of explicit coarse-grained equations. The coarse-grained behavior is analyzed directly, through appropriately designed short computational experiments by the fine-scale models. In the case of problems where the macroscopic behavior is characterized by scale invariance, dynamic renormalization [6, 7, 8], combined with equation-free computation and a template-based approach [9], can in effect convert the self-similar problem into a stationary one, by working in a frame of reference that expands or shrinks along with the macroscopic system observables.

Here we apply equation-free dynamic renormalization techniques to the problem of gravitational core collapse [10, 11]. A star cluster or galaxy evolves due to gravitational encounters between the stars, which drive the local velocity distribution toward a Maxwellian. Stars in the high-velocity tail of the Maxwellian escape from the system; the probability of escape in one relaxation time t_r ,

$$t_r \equiv \frac{0.065 v_m^3}{\rho m G^2 \ln \Lambda}, \quad (1)$$

is roughly 1%. Here v_m^2 is the mean square (3D) velocity of the stars, ρ is the mass density, m is the individual stellar mass, G is the gravitational constant, and

$\ln \Lambda \approx \ln(0.4N)$ is the Coulomb logarithm [2], with N the number of stars in the cluster. Escape occurs primarily from the high-density central region, or “core”; if the density contrast between core and envelope is sufficiently great, the core exhibits the negative specific heat characteristic of gravitationally bound systems [12] and contracts.

Treatments of core collapse based on fluid [13, 14] or Fokker-Planck [15, 16, 17] approximations to the full N -body equations of motion suggest that the late stages are self-similar,

$$\rho(r, t) \approx \rho_c(t) \rho_* \left[\frac{r}{r_c(t)} \right], \quad (2a)$$

$$\rho_c(t) = \rho_{c,0} (1 - t/t_{cc})^\gamma, \quad (2b)$$

$$r_c(t) = r_{c,0} (1 - t/t_{cc})^\delta, \quad (2c)$$

$$\rho_*(r) \rightarrow r^{-\alpha}, \quad r \gg r_c, \quad (2d)$$

with ρ_c and r_c the central density and core radius respectively, and t_{cc} the time at which the central density diverges; $t_{cc} - t$ is roughly 330 times the relaxation time of Eq. 1 if the latter is evaluated at the center of the cluster.

These predictions are in reasonable agreement with the results of direct N -body integrations [18, 19, 20]. But when N is finite, the number of particles in the core drops to zero as collapse proceeds, causing two-body and higher order correlations to dominate the evolution; typically, binary stars form which halt the collapse (“core bounce”). In all N -body simulations published to date, this occurs before or only shortly after the core has entered the self-similar regime. The rate of binary formation per unit volume due to three-body interactions is [21]

$$\dot{n}_{3-b} \approx 1.2 \times 10^2 \frac{G^5 m^2 \rho^3}{v_m^9}. \quad (3)$$

By the time that the number of stars in the core has dropped to N_c ($N_c \equiv \rho_c r_c^3$), the total number of binaries formed is $\sim 10^3 N_c^{-2}$. Since a single hard binary can

halt the collapse, bounce occurs when N_c has dropped to ~ 30 . This limits the maximum central density that can be reached in an N -body simulation to a multiple $\sim 10^{3.5}(N/10^4)^3$ of the initial density (assuming the initial state described below); for $N \approx 10^4$, the achievable density contrast is $\sim 10^4$, which is also roughly where self-similar behavior first appears [16].

In this paper, we exploit coarse dynamic renormalization to compute representative self-similar solutions at scales “away from” the latest stages of core collapse. This allows us to avoid the finite- N correlations that develop at those stages and recover features of the self-similar behavior predicted at the large- N limit. We define the “macroscopic” quantity of interest to be the single-particle distribution function $f(E)$, $E = v^2/2 + \Psi(r)$, with $\Psi(r)$ the self-consistent gravitational potential (spherical symmetry is assumed throughout). By dynamically renormalizing the N -body model after each short “burst” of integration, we are able to maintain a large ($\sim 10^3$) number of particles in the core even with modest ($\sim 16K$) total numbers, effectively halting binary formation and allowing us to accurately extract the form of the self-similar solution.

II. DESCRIPTION OF THE CALCULATIONS

We adopted the standard Plummer model [22] initial conditions for this problem, with density, gravitational potential, and single-particle distribution function given by

$$\begin{aligned} \rho(r) &= \frac{3}{4\pi} \frac{1}{(1+r^2)^{5/2}}, & \Psi(r) &= -\frac{1}{(1+r^2)^{1/2}}, \\ f(E) &= \frac{24\sqrt{2}}{7\pi^3} (-E)^{7/2}, & E &= v^2/2 + \Psi. \end{aligned} \quad (4)$$

Here and below, the gravitational constant G has been set to one. The N -body algorithm was an adaptation of S. J. Aarseth’s NBODY1 code [23] to the GRAPE-6 special-purpose computer and included a fourth-order particle advancement scheme with individual, adaptive, block time steps. We first used this code to carry out a direct integration until core bounce of a Plummer model with $N = 16384$ particles; the results (e.g. evolution of the central density, time of core bounce) agreed well with published studies using different N -body codes [18, 19, 20]. We used the same number of particles in the calculations described below.

Our coarse renormalization procedure consisted of short bursts of simulation in a “lift-simulate-restrict-rescale-truncate” procedure, repeated in a loop until the asymptotic form of the self-similar solution emerged. In detail, the steps were:

1. **Lift:** Given a smooth representation $\rho(r)$ of the density profile, a set of Monte-Carlo positions and velocities was generated, as follows. First an estimate of the gravitational potential $\Psi(r)$ was computed from $\rho(r)$

via Poisson’s equation. The isotropic, single-particle distribution function $f(E)$ corresponding to this density-potential pair is given uniquely by Eddington’s formula [24]. For the purposes of generating a new Monte-Carlo set of positions and velocities, the relevant function is not $f(E)$ but $N(<v, r)$, the cumulative number of stars with velocities less than v at radius r . Using Eddington’s formula, this can be shown to be

$$\begin{aligned} N(<v, r) &= 1 - \frac{1}{\rho} \int_0^E d\Psi' \frac{d\rho}{d\Psi'} \times \\ &\left\{ 1 + \frac{2}{\pi} \left[\frac{v/\sqrt{2}}{\sqrt{E-\Psi'}} - \tan^{-1} \left(\frac{v/\sqrt{2}}{\sqrt{E-\Psi'}} \right) \right] \right\}. \end{aligned} \quad (5)$$

2. **Integrate.** The N -body realization was advanced in time until the central density had increased by a factor of ~ 5 compared with the initial model. In the nearly-self-similar regime, this required approximately 250 central relaxation times.

3. **Restrict.** An estimate of $\rho(r)$ was computed from the particle coordinates $\mathbf{x}_i, i = 1 \dots N$ at the final time step. The position of the cluster center was first determined as in [25] and the particle radii r_i were defined with respect to this center. Each particle was then replaced by the kernel function

$$\begin{aligned} K(r, r_i, h_i) &= \frac{1}{2(2\pi)^{3/2}} \left(\frac{rr_i}{h_i^2} \right)^{-1} e^{-(r_i^2+r^2)/2h_i^2} \\ &\times \sinh(rr_i/h_i^2) \end{aligned} \quad (6)$$

which is an average over the sphere of radius r_i of the 3D Gaussian kernel of width h_i . The density estimate, $\rho(r) = \sum_{i=1}^N h_i^{-3} K(r, r_i, h_i)$, was then computed on a logarithmic radial grid. The kernel width h_i associated with the i th particle was determined by first constructing a pilot estimate of the density via a nearest-neighbor scheme, then allowing the h_i to vary as the inverse square root of this pilot density [26].

4. **Rescale:** The density estimate was rescaled, $\rho(r) \rightarrow A\rho(Br)$, according to an algorithm that left the core properties unchanged in the self-similar regime. The vertical normalization A was fixed by comparing the values of the density at $r = 0$ at the start and end of the integration interval. The radial scale factor B was adjusted such that the two density estimates had the same value at the radius where the density was $1/50$ of its central value.

5. **Truncate:** In the late stages of core collapse, the system develops a $\rho \sim r^{-\alpha}$, $\alpha \approx 2$ envelope around the shrinking core. In direct N -body integrations, this envelope grows to contain most of the total mass, and the number of stars in the core drops to zero, leading to the small- N effects discussed above. We avoided this by truncating the rescaled density beyond a radius $r_1 \approx 50r_c$ using a function that falls smoothly to zero at a radius $r_2 \approx 10r_1$.

6. Step 1 was then repeated in a loop.

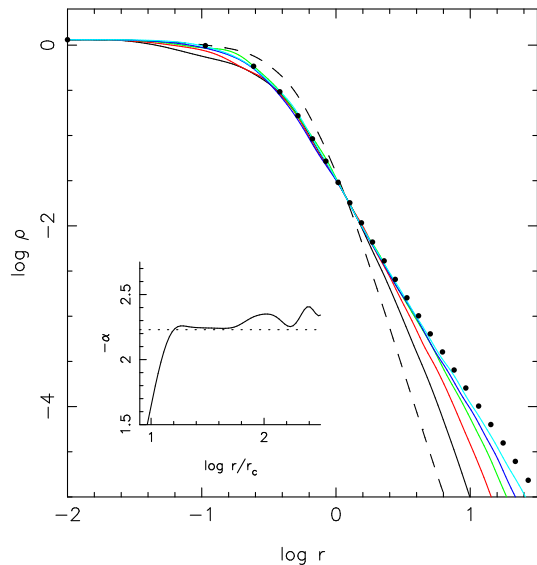


FIG. 1: Evolution of the rescaled density. Dashed line is the initial state and points are the self-similar $\rho_*(r)$ derived in Ref. [17]. Inset shows $\alpha \equiv -d \log \rho / d \log r$ at the end of the final integration; dashed line is $\alpha = -2.23$.

Generation of the new particle coordinates from the single-particle $f(E)$ in step 1 has the effect of removing any binaries that may have formed in the previous integration interval, and of resetting to zero any anisotropies that developed in the velocities. Since the number of particles in the core after each rescaling was $\sim 10^3$, the chance that even a single binary would form before the next rescaling was negligible. Velocity anisotropy was evaluated at the end of each interval and found to be very small, and restricted to the largest radii. The effects of binary formation and anisotropy growth could be reduced still more by increasing N and by reducing the lengths of the integration intervals. Newton-type fixed point algorithms that converge on the self-similar solution are also possible.

III. RESULTS

Fig. 1 shows the density profile at the end of each rescaling step, compared with the self-similar $\rho_*(r)$ computed from the orbit-averaged isotropic Fokker-Planck equation [17], which has $\rho_* \propto r^{-2.23}$ at large radii. The renormalized density is quite close to the self-similar solution after 4-5 iterations.

In the self-similar regime, the finite changes in central density and core radius during one integration interval satisfy $\log(\rho_{c,f}/\rho_{c,i})/\log(r_{c,f}/r_{c,i}) = \gamma/\delta$; in the Fokker-Planck approximation [17], this ratio is equal to the asymptotic density slope, $\gamma/\delta = \alpha \approx -2.23$. We computed this ratio from the rescaling factors (A, B) in each integration interval and found it to be $(-2.09, -2.15, -2.23, -2.24, -2.23, -2.23)$, consistent

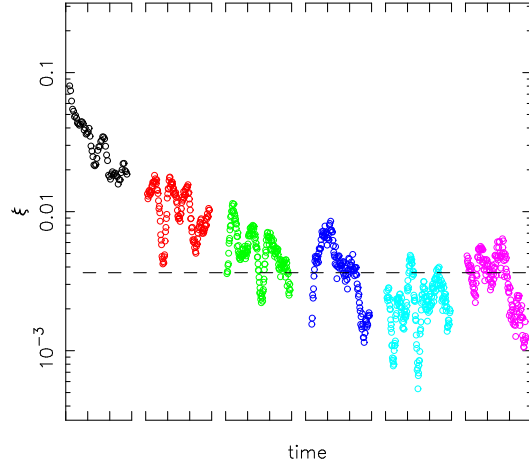


FIG. 2: Evolution of the dimensionless collapse rate parameter $\xi \equiv (\dot{\rho}_c/\rho_c)/t_r$. Each time interval corresponds to one “burst” of integration, after which the model was rescaled as described in the text. Dashed line shows the asymptotic (self-similar) value $\xi = 3.6 \times 10^{-3}$ as computed via the isotropic orbit-averaged Fokker-Planck equation [16, 17].

with the Fokker-Planck prediction at late times, and also consistent with our computed value of α (Fig. 1).

The dimensionless collapse rate is

$$\xi \equiv t_r(0) \frac{1}{\rho_c} \frac{d\rho_c}{dt} \quad (7)$$

with $t_r(0)$ the value of the relaxation time (Eq. 1) evaluated at $r = 0$; in the self-similar regime, ξ should reach a constant value. Fig. 2 shows the evolution of ξ , computed by fitting a smoothing spline to $\rho_c(t)$ during each of the integration intervals. Isotropic Fokker-Planck treatments [16, 17] find $\xi \approx 3.6 \times 10^{-3}$ in the self-similar regime, consistent within the noise with Fig. 2.

Another way to measure the degree of evolution achieved via the rescaled integrations is shown in Fig. 3. In this plot, the cumulative effect of the rescalings on ρ_c and r_c is included; the central density has increased by a cumulative factor of $\sim 10^{4.5}$ by the end of the fifth rescaling, and the core radius has decreased by a factor $\sim 10^2$. The $\rho_c(r_c)$ relation from the N -body integration without rescaling is also shown. In the un-rescaled integration, the central density peaks due to binary formation at a value ~ 10 times lower than in the rescaled runs.

In principle, one can extract the similarity exponents γ and δ of Eq. 2 (not just their ratio) from the numerical models. For instance, if t_1 and t_2 are two distinct times in the self-similar regime, then

$$\gamma = \frac{t_2 - t_1}{\frac{\rho_c(t_2)}{d\rho_c/dt|_{t_2}} - \frac{\rho_c(t_1)}{d\rho_c/dt|_{t_1}}} \quad (8)$$

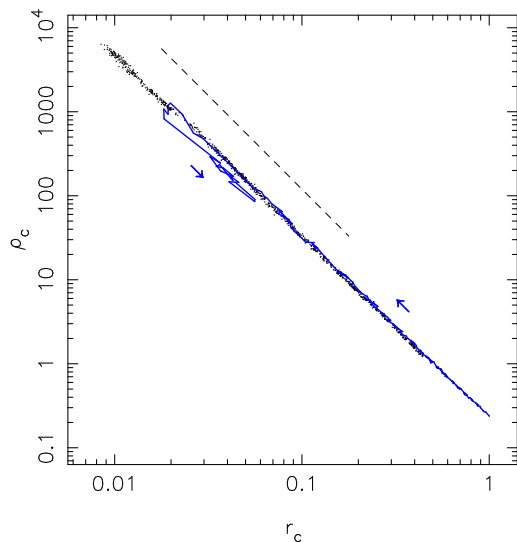


FIG. 3: Central density vs core radius in the rescaled runs (points) and in a direct N -body integration (blue line). Dashed line shows $\rho_c \propto r_c^{-2.23}$. In the direct N -body simulation without rescaling, the central density reaches a peak value then decreases (“core bounce”) due to formation of binary stars.

and similarly for δ . Another approach [9] is via numerical calculation of the scaling exponents that characterize the effective differential operator. A third approach is simply to fit Eqs. 1 to the time-dependent density and core radius in the self-similar regime. We had limited success with each of these methods due to noise associated with the modest particle numbers. The noise could be reduced by averaging the results from different random realizations of the same initial conditions, or by increasing N .

IV. CONCLUSIONS

Coarse dynamic renormalization is a tool for numerically extracting self-similar solutions by evolving a dy-

namical system to a stationary state, in a scaled reference frame where the self similarity has been “factored out.” We have demonstrated the usefulness of the method for studying gravitational core collapse. In the limit of large particle numbers, core collapse is characterized by a central density that increases without limit, due to the combined effects of heat transfer and the negative specific heat of the core. In numerical simulations with finite N , collapse is halted when the number of particles in the shrinking core drops to a small enough value that binaries can form. By carrying out short bursts of integration of appropriately rescaled initial conditions, we showed that it is possible to avoid these small- N effects and to follow collapse well into the self-similar regime. Furthermore we achieved this with quite modest particle numbers, $N \approx 10^4$. In our approach, the degree to which core collapse can be followed is essentially independent of the number of particles used, while in direct N -body simulations, the time to core bounce is determined by N .

We chose the macroscopic function of interest to be the isotropic, single-particle distribution function $f(E, t)$. The same approximation is commonly made in Fokker-Planck and fluid treatments of core collapse [13, 16, 17]. A larger particle number would allow us to relax the assumption of isotropy and extract $f(E, L, t)$ with L the orbital angular momentum per unit mass. Results so obtained could be compared with solutions to the anisotropic Fokker-Planck [15, 27, 28] and fluid [14] equations.

Acknowledgments

This work was supported by grants AST-0206031, AST-0420920, AST-0437519, and CTS-0205484 from the NSF, grants NNG04GJ48G and NAG 5-10842 from NASA, and grant HST-AR-09519.01-A from STScI.

-
- [1] S. J. Aarseth, *Gravitational N-body simulations* (Cambridge, Cambridge University Press, 2003, 506 p., 2003).
 - [2] L. Spitzer, *Dynamical evolution of globular clusters* (Princeton, NJ, Princeton University Press, 1987, 191 p., 1987).
 - [3] C. Gear, I. Kevrekidis, and K. Theodoropoulos, *Computers and Chemical Engineering* **26**, 941 (2002).
 - [4] I. Kevrekidis, C. Gear, J. Hyman, P. Kevrekidis, O. Runborg, and K. Theodoropoulos, *Comm. Math. Sci.* **1**, 715 (2003).
 - [5] I. Kevrekidis, C. Gear, and G. Hummer, *A. I. Ch. Eng. Journal* **50**, 1346 (2004).
 - [6] D. W. McLaughlin, G. C. Papanicolaou, C. Sulem, and P. L. Sulem, *Phys. Rev. A* **34**, 1200 (1986).
 - [7] B. J. Lemesurier, G. Papanicolaou, C. Sulem, and P. L. Sulem, *Physica D Nonlinear Phenomena* **31**, 78 (1988).
 - [8] B. J. Lemesurier, G. C. Papanicolaou, C. Sulem, and P. L. Sulem, *Physica D Nonlinear Phenomena* **32**, 210 (1988).
 - [9] C. W. Rowley, I. G. Kevrekidis, J. E. Marsden, and K. Lust, *Nonlinearity* **16**, 1257 (2003).
 - [10] M. Hénon, *Annales d’Astrophysique* **24**, 369 (1961).
 - [11] M. Hénon, *Annales d’Astrophysique* **28**, 62 (1965).
 - [12] D. Lynden-Bell and R. Wood, *Mon. Not. R. Astron. Soc.*

- 138**, 495 (1968).
- [13] D. Lynden-Bell and P. P. Eggleton, *Mon. Not. R. Astron. Soc.* **191**, 483 (1980).
- [14] P. D. Louis and R. Spurzem, *Mon. Not. R. Astron. Soc.* **251**, 408 (1991).
- [15] H. Cohn, *Astrophys. J.* **234**, 1036 (1979).
- [16] H. Cohn, *Astrophys. J.* **242**, 765 (1980).
- [17] D. C. Heggie and D. Stevenson, *Monthly Notices of the Royal Astronomical Society* **230**, 223 (1988).
- [18] R. Spurzem and S. J. Aarseth, *Mon. Not. R. Astron. Soc.* **282**, 19 (1996).
- [19] J. Makino, *Astrophys. J.* **471**, 796 (1996).
- [20] H. Baumgardt, D. C. Heggie, P. Hut, and J. Makino, *Mon. Not. R. Astron. Soc.* **341**, 247 (2003).
- [21] P. Hut, in *IAU Symp. 113: Dynamics of Star Clusters* (1985), pp. 231–247.
- [22] H. C. Plummer, *Mon. Not. R. Astron. Soc.* **71**, 460 (1911).
- [23] S. J. Aarseth, *Pub. Astron. Soc. Pac.* **111**, 1333 (1999).
- [24] A. S. Eddington, *Mon. Not. R. Astron. Soc.* **76**, 572 (1916).
- [25] S. Casertano and P. Hut, *Astrophys. J.* **298**, 80 (1985).
- [26] B. W. Silverman, *Density Estimation for Statistical and Data Analysis* (London, England, Chapman and Hall, 1986, 000 p., 1986).
- [27] K. Takahashi, *Pub. Astron. Soc. Japan* **47**, 561 (1995).
- [28] K. J. Joshi, F. A. Rasio, and S. Portegies Zwart, *Astrophys. J.* **540**, 969 (2000).